

Crystal Structure of the Clathrate Form of Syndiotactic Poly(*p*-methylstyrene) Containing Tetrahydrofuran

Vittorio Petraccone, Domenico La Camera, Beniamino Pirozzi, Paola Rizzo, and Claudio De Rosa*

Dipartimento di Chimica Università di Napoli "Federico II", Via Mezzocannone 4, 80134 Napoli, Italy

Received December 30, 1997; Revised Manuscript Received June 2, 1998

ABSTRACT: The crystal structure of the clathrate form of syndiotactic poly(*p*-methylstyrene) containing tetrahydrofuran is presented. Polymer chains in the $s(2/1)2$ helical conformation and molecules of tetrahydrofuran are packed in the monoclinic unit cell with axes $a = 18.8$ Å, $b = 12.7$ Å, and $c = 7.7$ Å, and with $\gamma = 100^\circ$ according to the space group $P2_1/a$. Two polymer chains (eight monomer units) and four molecules of tetrahydrofuran are included in the unit cell. The calculated crystalline density is 1.13 g/cm³. Tetrahydrofuran molecules occupy cavities delimited by the benzene rings of adjacent polymer chains along the b axis; each cavity is occupied by two molecules of tetrahydrofuran related by the 2-fold screw axis. A comparison with the crystal structures of the clathrate forms of syndiotactic polystyrene is presented.

Introduction

The complex polymorphic behavior of syndiotactic poly(*p*-methylstyrene) (s-PPMS) has been recently described.^{1,2} Four different crystalline forms (forms I, II, III, and V), a mesomorphic form (form IV), and several clathrate forms have been found so far.^{1,2} The clathrate forms correspond to structures where polymer chains (the host) form a crystal lattice containing spaces in which molecules of a second chemical species (the guest) are located.

X-ray fiber diffraction data of the various crystalline forms of s-PPMS,² as well as solid state ¹³C NMR³ and FTIR⁴ studies have shown that the chains of s-PPMS assume trans planar or $s(2/1)2$ helical conformation. In particular, forms I and II and all clathrate forms are characterized by chains in the $s(2/1)2$ helical conformation, whereas forms III, IV, and V present chains in the trans planar conformation. Only the crystal structure of form III has been solved so far;⁵ trans planar chains are packed in an orthorhombic unit cell with axes $a = 13.36$ Å, $b = 23.21$ Å, and $c = 5.12$ Å according to the space group $Pnam$.⁵

Clathrate structures have been also found for syndiotactic polystyrene (s-PS).^{6–11} Although the intensities and the precise locations of reflections in the X-ray diffraction patterns of these clathrate forms of s-PS change with the kind and the amount of the included guest molecules,^{6,7} only one kind of clathrate structure (δ form⁷) has been found so far for s-PS. Indeed, the crystal structures of clathrate δ forms of s-PS including molecules of toluene,⁸ iodine,⁹ and 1,2-dichloroethane,¹¹ recently described, are characterized by the same crystal monoclinic symmetry (space group $P2_1/a$) and similar dimensions of the unit cells.

Two different classes of clathrate forms have been instead described for s-PPMS.¹² Indeed, clathrate forms containing *o*-dichlorobenzene, *o*-chlorofenol, *o*-xylene, and *N*-methyl-2-pyrrolidone have similar X-ray diffraction patterns; they have been called α class clathrates.¹² Clathrate forms of s-PPMS containing tetrahydrofuran, benzene, cyclohexane, cyclohexanone, and 1,4-dioxane have similar X-ray diffraction patterns that are different

with respect to those of the α class. They have been called β class clathrates.¹² α class and β class clathrates are transformed into forms I and II of s-PPMS, respectively, by suitable treatments involving removal of the guest molecules, like annealing^{1,2,12} or treatments with acetone.¹²

In this paper the crystal structure of the clathrate form of s-PPMS containing tetrahydrofuran (THF) is presented. This structure could be considered as representative of the crystal structure of the β class clathrates of s-PPMS.

Experimental Part and Method of Calculation

s-PPMS was synthesized with a homogeneous catalytic system, composed of tetrabenzyltitanium and methylaluminumoxane, as described in ref 1. The syndiotacticity of the polymer was evaluated by ¹³C NMR; the fraction of *rrrr* pentads was higher than 95%.

Unoriented samples of the clathrate form of s-PPMS containing THF were obtained by casting procedures from 10 wt % THF solution at room temperature. Oriented fibers of the clathrate form were obtained by exposing fiber samples in the mesomorphic form IV to THF vapor for 1 min at room temperature under conditions of fixed length.² Fibers of the mesomorphic form IV were obtained by stretching films of s-PPMS in form I at 130 °C.^{1,2} Films of s-PPMS in form I were obtained by casting procedures from 10 wt % toluene solution at 50 °C.

The drawing of s-PPMS films was conducted with a Minimat apparatus with a strain rate of $0.1\text{--}0.2$ min^{−1}.

Wide-angle X-ray diffraction patterns were obtained with nickel-filtered Cu K α radiation. The diffraction patterns of oriented samples were obtained with a photographic cylindrical camera, whereas those for unoriented samples were recorded with an automatic Philips diffractometer.

The thermogravimetric analyses were carried out from room temperature to 250 °C with a Mettler TG50 thermobalance in a flowing-nitrogen atmosphere at a heating rate of 10 K/min. In this range of temperature no decomposition of the sample occurs.

Calculated X-ray fiber diffraction intensities were obtained from the calculated structure factors F_c as $I_c = |F_c|^2 MLP$, where M is the multiplicity factor and LP is the Lorentz–polarization factor for X-ray fiber diffraction: $LP = (1 + \cos^2 2\theta)/[2(\sin^2 2\theta - \zeta^2)^{1/2}]$, with $\zeta = \lambda/lc$, l and c being the order of the layer line

and the chain axis, respectively. A thermal factor $B = 8 \text{ \AA}^2$ and atomic scattering factors from ref 13 were used.

The calculated X-ray powder diffraction profile ($I_{\text{calc},2\theta_i}$) was obtained from the calculated diffraction intensities I_{hkl} of the hkl reflections as

$$I_{\text{calc},2\theta_i} = \sum I_{hkl} \Omega(2\theta_i - 2\theta_{hkl})$$

where the sum is extended over all hkl reflections with Bragg angles $2\theta_{hkl}$ close to the profile point $2\theta_i$ and $\Omega(2\theta_i - 2\theta_{hkl})$ is a proper profile function. A Gauss profile function having a half-height width regulated by the function $H = [U \tan^2 \theta + V \tan \theta + W]^{1/2}$ was used. The parameters U , V , and W were optimized in order to reproduce the half-height width of the peaks in the experimental profile. The diffraction intensities I_{hkl} were obtained from the calculated structure factors F_{hkl} as $I_{hkl} = |F_{hkl}|^2 MLP$, where M is the multiplicity factor and LP is the Lorentz-polarization factor for X-ray powder diffraction: $LP = (1 + \cos^2 2\theta)/2 \sin^2 \theta \cos \theta$.

A quantitative comparison between calculated and experimental intensities was performed by evaluating the experimental intensities from the X-ray powder diffraction pattern. The experimental intensities I_o were obtained by measuring the area of the peaks in the X-ray powder pattern after the subtraction of the amorphous halo. The agreement R factor has been calculated as $R = \sum |I_o - I_c| / \sum I_o$ with $I_c = \sum I_{hkl}$, where the summation is taken over all reflections included in the 2θ range of the corresponding observed reflection peak.

The calculations of the packing energy were performed with the parameters for the nonbonded energy reported by Flory,¹⁴ taking the methyl groups as single rigid units.¹⁵ The conformations of the polymeric chain and of the THF molecules were kept constant, and the interactions were calculated within spheres of radii equal to twice the sum of the van der Waals radii for each pair of atoms. The values of the conformational parameters of the s-PPMS chain were obtained by performing minimizations of the internal energy of the isolated chain by using the potential functions and the method described in ref 16 for s-PS. The parameters for the nonbonded energy are the same as used in the packing energy calculations. At variance with calculations of ref 16, in these minimizations we have varied independently the bond angles of two adjacent methylene carbon atoms. Torsion and bond angles of the THF molecule were found by performing minimizations of the internal energy of the isolated molecule by using the program AMBER.¹⁷

Results and Discussion

Unit Cell, Space Group, and THF Content Determination. The X-ray fiber diffraction pattern of the clathrate form of s-PPMS containing THF is reported in Figure 1. Fiber and powder samples of the clathrate form present a density, measured by flotation, of 1.02 g/cm^3 . All the reflections observed in the fiber pattern are listed in Table 1. The reflections were indexed in terms of a monoclinic unit cell with cell constants $a = 18.8 \text{ \AA}$, $b = 12.7 \text{ \AA}$, $c = 7.7 \text{ \AA}$, and $\gamma = 100^\circ$. The space group is $P2_1/a$, in agreement with the systematic absences of $hk0$ reflections with $h = 2n + 1$.

Thermogravimetric measurements on powder samples, obtained by casting from THF solutions and showing an X-ray crystallinity index of nearly 50%, indicate weight losses in the range 13–15%. Indeed, the amount of the guest molecules included in the crystalline and amorphous phases depends on the sorption as well as desorption (and storage) conditions. Samples of s-PPMS, prepared with a similar procedure but showing no significant X-ray crystallinity, present weight losses in the range 9–10%, if the thermogravimetric measurements are performed just after the preparation of the samples. The weight loss decreases rapidly if the

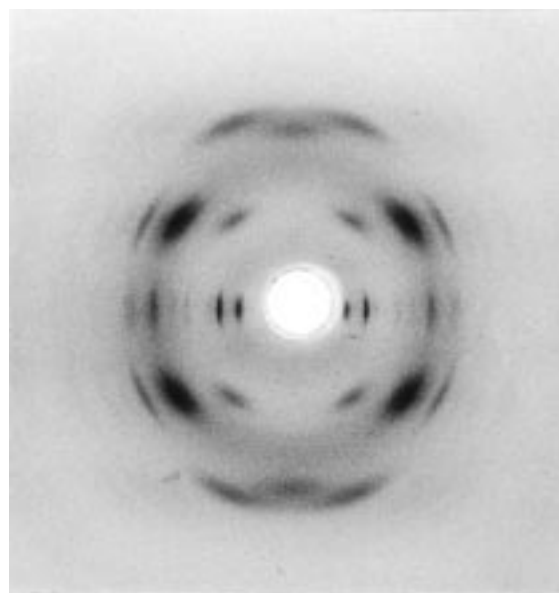


Figure 1. X-ray fiber diffraction pattern of the clathrate form of s-PPMS containing tetrahydrofuran.

Table 1. Diffraction Angles 2θ , Bragg Distances d , Reciprocal Coordinates ξ and ζ , and Intensities I_{obs} of the Reflections Observed on the Layer Lines l of the X-ray Fiber Diffraction Pattern of the Clathrate Form of s-PPMS Containing Tetrahydrofuran (Figure 1)

2θ (deg)	d (Å)	ξ (Å ⁻¹)	ζ (Å ⁻¹)	l	I_{obs}^a
7.0	12.6	0.080	0	0	m
9.6	9.19	0.109	0	0	s
10.9	8.12	0.124	0	0	vvw
14.0	6.33	0.158	0	0	w
15.6	5.68	0.177	0	0	vw
18.4	4.82	0.208	0	0	ms
21.25	4.18	0.238	0	0	m
13.9	6.37	0.090	0.130	1	s
18.1	4.90	0.160	0.130	1	ms
19.1	4.65	0.173	0.130	1	vs
20.5	4.33	0.192	0.130	1	m
22.5	3.95	0.218	0.130	1	s
24.7	3.60	0.246	0.130	1	w
26.6	3.35	0.270	0.130	1	w
30.0	2.98	0.310	0.130	1	vw
22.3	3.99	0.	0.246	2	ne
25.0	3.56	0.126	0.251	2	s
27.1	3.28	0.173	0.251	2	vvvw
29.3	3.05	0.212	0.251	2	vw
31.4	2.85	0.246	0.251	2	vvw

^a vs = very strong, s = strong, ms = medium strong, m = medium, w = weak, vw = very weak, vvw = very very weak, ne = not evaluated.

samples are left at room temperature for several days (after 1 day the weight loss is 7–8%). These amorphous samples containing 9–10% of THF present a density of 0.95 g/cm^3 , lower than that of amorphous samples of s-PPMS obtained by cooling the melt to room temperature (1.02 g/cm^3). On the basis of these data we concluded that the molar ratio monomer/THF in the semicrystalline samples of the clathrate form of s-PPMS with THF should be close to 2. The calculated crystalline density is 1.13 g/cm^3 assuming two chains of s-PPMS in the $s(2/1)_2$ helical conformation and four THF molecules included in the unit cell (molar ratio monomer/THF equal to 2).

Packing Models of only s-PPMS Chains. To find possible packing models of s-PPMS chains, showing cavities that are able to accommodate THF molecules, calculations of the packing energy of only s-PPMS

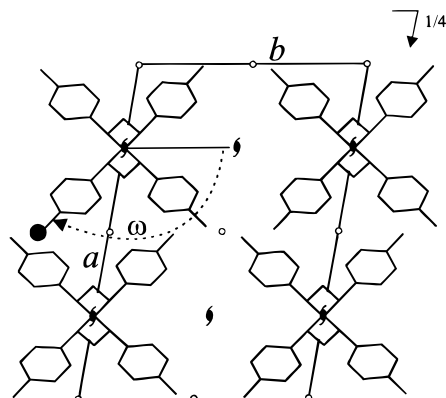


Figure 2. Definitions of the variables used in the packing energy calculations of the only s-PPMS chains. ω is the rotation angle of the $s(2/1)2$ helical chain of s-PPMS around the chain axis; it is positive for a clockwise rotation. The height of the carbon atom indicated by a filled circle defines the z coordinate. The crystallographic symmetry elements of the space group $P2_1/a$ are also shown. The orientation of the chains of s-PPMS in the unit cell corresponds to the absolute packing energy minimum of the map of Figure 3A ($\omega = 132.7^\circ$).

chains, without the guest molecules, were performed. The s-PPMS chains were positioned in the unit cell with their 2-fold screw axes coincident with the crystallographic 2-fold screw axes in the space group $P2_1/a$. The values of the conformational parameters of the $s(2/1)2$ helical chains of s-PPMS were obtained by performing minimizations of the internal energy of the isolated chain. The bond distances are C–C = 1.54 Å, C–C_{ar} = 1.51 Å, C_{ar}–C_{ar} = 1.39 Å, C–H = 1.10 Å, and C_{ar}–H = 1.08 Å. The bond angle on the methine carbon atoms is 111.6° , whereas those on the two methylene carbon atoms belonging to two successive monomeric units are 114.0 and 116.0° ; the two torsion angles, for a left-handed $s(2/1)2$ helical symmetry, are $+179.8$ and -63.6° . The phenyl ring is positioned with its plane bisecting the bond angle on the methine carbon atom.

Packing energy calculations were performed by maintaining the parameters of the unit cell constant at the experimental values and varying the orientation (ω) and the height (z) of the chain having the chain axis positioned at $x = 0.25, y = 0$. The angle of rotation ω of the chain around its axis and the height z are defined in Figure 2. A map of the packing energy for the space group $P2_1/a$, calculated as half the sum of the interaction energies between the atoms of one monomeric unit and all the surrounding atoms of the neighboring macromolecules, is reported as a function of ω and z/c in Figure 3A. The map is periodic over $\omega = 180^\circ$ and $z/c = 0.5$; therefore, only the portion of the map in the range $\omega = 0-180^\circ$ and $z/c = 0-0.5$ is shown. The map presents two nearly isoenergetic minima of lower energy and other minima of higher energy. The analysis of the empty spaces in the packing models corresponding to the energy minima of Figure 3A has shown that only for the absolute energy minimum model (shown in Figure 2, $\omega = 132.7^\circ, z/c = 0.220$) the chains of s-PPMS are arranged so that there is plenty of space for including the guest THF molecules. In this model (Figure 2) there are empty spaces around the 2-fold screw axes of the lattice located at $x/a = 0.25, y/b = 0.5$ and $x/a = 0.75, y/b = 0.5$. Each cavity is able to accommodate up to two THF molecules related by the 2-fold screw axis. This is in agreement with the previous considerations about the crystalline density and the thermogravimetric measurements.

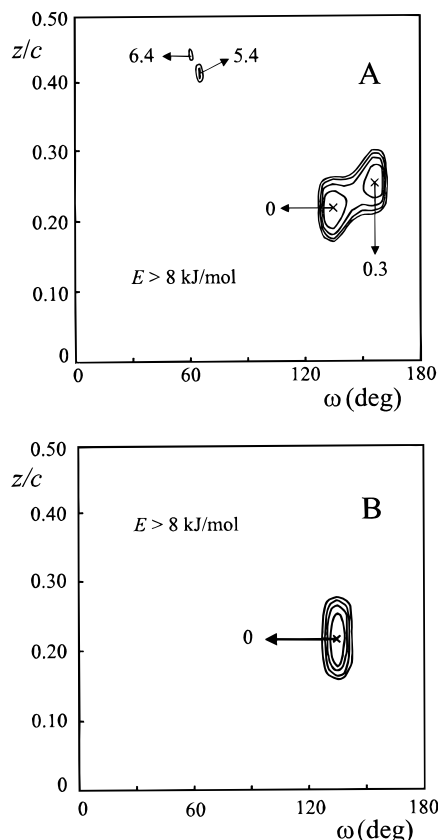


Figure 3. Maps of the packing energy of s-PPMS chains without (A) and with (B) the guest molecules as a function of ω and z/c for the space group $P2_1/a$. In part B the s-PPMS chain and the THF molecule are considered as a rigid unit, the position and the conformation of THF are fixed as in Figures 5A and 6A, and ω and z are defined as in Figure 2 but in this case refer to the couple polymer chain–THF molecule. In both maps the curves are drawn at intervals of 2 kJ/mol with respect to the absolute minimum of each map assumed as zero.

Positioning of the THF Molecules. With the assumption that each cavity contains two THF molecules related by the 2-fold screw axis, it is easily realized that the position of each THF molecule inside the cavity is regulated by the interactions of the THF molecule with the closest polymer chain. Hence calculations of the nonbonded interaction energy between one chain of s-PPMS and one THF molecule were performed. The energy was calculated as half the sum of the interaction energy between the atoms of a THF molecule and all the atoms of the s-PPMS chain. The conformation of the chain and of the THF molecule was maintained constant. In these calculations we assumed that the THF molecule was in the stable half-chair conformation having a C_2 symmetry,¹⁸ and arranged with its 2-fold symmetry axis coincident with the local 2-fold axis of the $s(2/1)2$ helical chain of s-PPMS, perpendicular to the chain axis and crossing the polymer methylene carbon, as shown in Figure 4. The torsion and bond angles of THF in the half-chair conformation were obtained by performing minimization of the internal energy of the isolated THF molecule. Owing to the chirality of the s-PPMS helical chain, both enantiomorphous half-chair conformations of the THF molecule (called I and I' in the following) were considered. The torsion angles of the THF molecule in the conformation I are C–O–C–C = -11° , O–C–C–C = 29° , and C–C–C–C = -35° ; those for the conformation I' are the same but with opposite sign. Two different orientations of

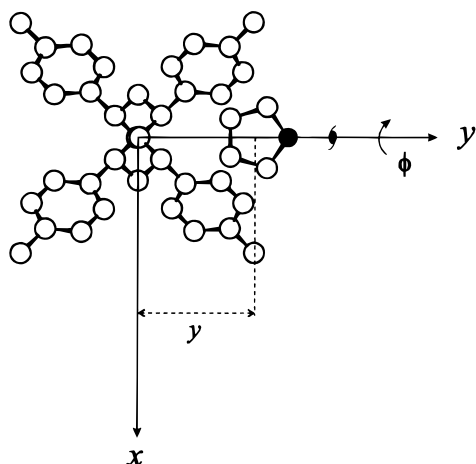


Figure 4. Definition of the coordinates used in the calculations of the interaction energy between one chain of s-PPMS and one THF molecule. y is the distance between the chain axis and the barycenter of the THF molecule. ϕ is the angle of rotation (positive for a clockwise rotation) of the THF molecule around its 2-fold rotation axis. The 2-fold rotation axis of the THF molecule and the 2-fold rotation axis of the s-PPMS chain, perpendicular to the chain axis and crossing the methylene carbon, are coincident with the y axis. The oxygen atom of the THF molecule is indicated by the filled circle.

the THF molecules depending on the position of the oxygen atom, which can be pointed toward the polymer chain or the 2-fold screw axis (see Figure 4), were considered. With these assumptions, and by maintaining the orientation of the s-PPMS chain constant, the x and z coordinates of the barycenter of the THF molecule in the frame of Figure 4 are defined. Hence, the position of the THF molecule in the frame of Figure 4 depends on only two variables: the distance between the barycenter of the THF molecule and the chain axis of the s-PPMS chain (y coordinate in Figure 4) and the rotation angle of the THF molecule around its 2-fold rotation axis (ϕ in Figure 4). If $\phi = 0^\circ$, the mean plane of the THF molecule in the half-chair conformation is parallel to the xy plane in the frame of Figure 4 (hence to the ab plane of the unit cell).

Lowest values of the energy are obtained, for both conformations I and I', when the THF molecule is oriented with the oxygen atom pointing toward the 2-fold screw axis. For the two conformations I and I' of THF, two nearly isoenergetic minima are obtained for different values of y and ϕ . For the conformation I the absolute energy minimum ($E = -54.8$ kJ/mol) is obtained for $y = 4.56$ Å when the mean plane of the THF molecule is nearly parallel to the ab plane of the unit cell ($\phi = 5^\circ$), whereas for the conformation I' the energy minimum ($E = -51.2$ kJ/mol) is obtained for $y = 4.76$ Å when the THF molecule is rotated by $\phi = -43^\circ$. The two different orientations of the THF molecule, corresponding to the energy minima are shown in Figure 5A,B, for the conformations I and I', respectively. The xz projections of the models of Figure 5 are also reported in Figure 6A,B in order to show the effective space available for the accommodation of the THF molecule between the benzene rings of a single s(2/1)2 helical chain of s-PPMS.

Final Model and Structure Factor Calculations.

To find the best position of the s-PPMS chains and of the THF molecules inside the unit cell, calculations of the packing energy (already shown for polymer chains without THF) of the polymer chains and guest molecules

Table 2. Fractional Coordinates of the Atoms of the Asymmetric Unit in the Model of Figure 7 for the Clathrate Form of s-PPMS with THF^a

	x/a	y/b	z/c
C1	0.250	0.004	0.475
C2	0.204	0.057	0.349
C3	0.161	-0.025	0.225
C4	0.206	-0.082	0.102
C5	0.153	0.116	0.445
C6	0.158	0.225	0.424
C7	0.111	0.279	0.513
C8	0.059	0.224	0.623
C9	0.054	0.114	0.643
C10	0.101	0.060	0.555
C11	0.007	0.282	0.719
C12	0.157	-0.170	0.006
C13	0.105	-0.144	-0.107
C14	0.059	-0.224	-0.196
C15	0.066	-0.331	-0.171
C16	0.118	-0.356	-0.057
C17	0.163	-0.276	0.031
C18	0.016	-0.418	-0.267
C19	0.309	0.408	-0.038
O20	0.245	0.453	-0.025
C21	0.182	0.372	-0.011
C22	0.207	0.267	-0.054
C23	0.286	0.289	0.005

^a The asymmetric unit corresponds to the two monomeric units and the atoms of THF labeled in Figure 7.

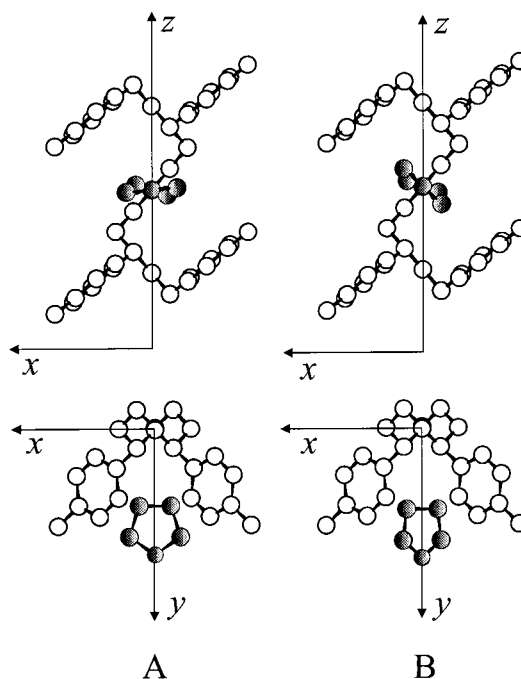


Figure 5. Two different orientations of the THF molecule with respect to the s(2/1)2 left-handed helical chain of s-PPMS corresponding to the minima of the interaction energy, for the THF in the half-chair conformations I (A) and I' (B). Only the four phenyl rings close to the THF molecule are shown.

were performed. Owing to the assumption of the coincidence of the local 2-fold rotation axes of s-PPMS and THF molecules, the polymer chain and the THF molecule were considered as a rigid unit and the packing energy was calculated as the interaction energy between the atoms of the couple polymer chain-THF molecule and all the surrounding atoms of the neighboring macromolecules and guest THF molecules. The energies were divided by 4 to allow a comparison with the energies of the map of Figure 3A, where the packing energies of the only s-PPMS chains were calculated with

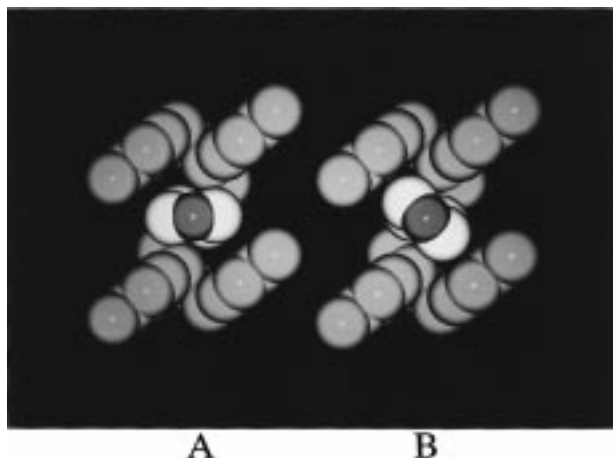


Figure 6. xz projections of the models of Figure 5 showing the van der Waals encumbrance of the atoms and the effective space available for the accommodation of the THF molecule in the half-chair conformations I (A) and I' (B). Carbon and oxygen atoms of the THF molecule are indicated with white and gray circles, respectively. Carbon atoms of the polymer chain are indicated with light gray circles.

respect to one monomeric unit. Only the results for the couple polymer chain–THF molecule of Figures 5A and 6A, corresponding to the lowest energy and to the conformation I of THF, are shown. Packing energy calculations were also performed for the couple polymer chain–THF molecule of Figures 5B and 6B, corresponding to the conformation I' of THF, but no significant changes were observed. The calculations were performed by varying the orientation ω of the couple polymer chain–THF molecule around the chain axis and the z/c coordinate that defines the relative heights of the couples polymer chain–THF molecule in the unit cell, as in the case of the packing energy calculations of the s-PPMS chains alone (see Figure 2). A map of the packing energy as a function of ω and z/c is reported in Figure 3B. Only one packing energy minimum is present in the map of Figure 3B at $\omega = 134.1^\circ$ and $z/c = 0.219$. This minimum is very close to one of the two nearly isoenergetic minima present in the map of the packing energy of the only s-PPMS chains of Figure 3A. The second minimum present in the map of Figure 3A (at $\omega = 160^\circ$ and $z/c = 0.267$) disappears in the calculations of Figure 3B performed by including the guest molecules, indicating that in the model of packing corresponding to this energy minimum for the s-PPMS chains there is no abundance of space in the unit cell for including two guest THF molecules.

Structure factor calculations, performed for the model of packing corresponding to the absolute minimum of the map of Figure 3B, show a good agreement with the experimental intensities observed in the X-ray fiber diffraction pattern of Figure 1. Structure factor calculations for different packing models corresponding to various points inside the minimum of the map of Figure 3B have shown no significant improvement of the agreement. The intensities of the reflections in the X-ray diffraction patterns depend on changes in THF content, as well as on the presence of possible disorder in the positioning of THF molecules inside the cavities. Structure factor calculations have been also performed by varying the occupancy factors of the atoms of the THF molecule. The best agreement is obtained when the occupancy factors are close to 1, indicating that in the ideal structure two THF molecules are included in

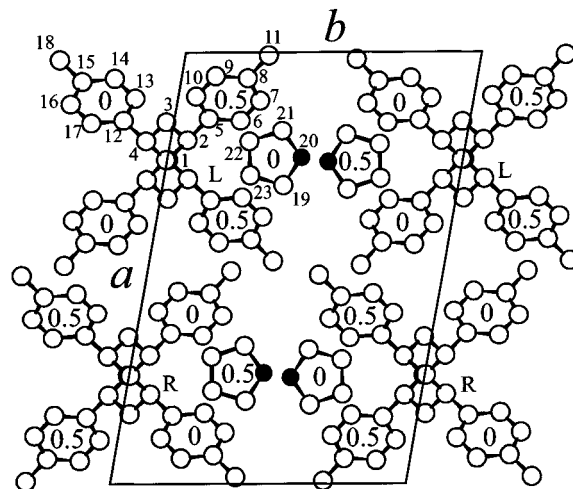


Figure 7. Model of packing for the crystal structure of the clathrate form of s-PPMS containing THF in the space group $P2_1/a$. The atoms of the asymmetric unit are labeled. The oxygen atoms of the THF molecules are indicated by filled circles. The approximate z/c fractional coordinates of the phenyl rings and THF molecules are also shown. R = right-handed chain, L = left-handed chain.

each cavity. Moreover, structure factor calculations, performed for models with low packing energy and the THF molecule in the conformation I' oriented as in Figures 5B and 6B, show no significant change of the agreement. In addition, the possibility that the THF molecule could also be in other low-energy conformations, like for instance, the envelope conformation,¹⁸ cannot be excluded. This indicates that the X-ray diffraction data are probably a representation of an average positioning of the THF molecules, which can assume in the cavities different low-energy conformations.

The model of packing of the clathrate form of s-PPMS containing THF corresponding to the absolute minimum of the map of Figure 3B ($\omega = 134.1^\circ$, $z/c = 0.219$, $y = 4.56$ Å, $\phi = 5^\circ$), which gives the best agreement, is shown in Figures 7 and 8 in the ab and $cb \sin \gamma$ projections, respectively.

The crystal structure is characterized by a close packing of right- and left-handed helical chains alternating along the a axis, where most of the carbon atoms of the side groups come into contact at the van der Waals distances (the shortest intermolecular distance between carbon atoms of adjacent chains along a is 3.7 Å). On the contrary, along the b axis a very loose packing of the polymer chains is achieved. Indeed, apart from the contact distance of 3.8 Å between the methyl carbons of the two adjacent chains, all contact distances between the phenyl carbons are greater than 5.7 Å and the shortest distance between the methyl and phenyl carbons of adjacent chains is 4.8 Å. This indicates the presence, along b , of space to accommodate the THF molecules. The shortest distance between the atoms of the two THF molecules is 4.0 Å, and the shortest distance between the atoms of the polymer chain and the THF molecule is 3.7 Å. It is apparent from Figure 8 that the space between adjacent chains along the b axis occupied by two THF molecules may be considered as composed of two separate cavities, each delimited by four benzene rings of one polymer chain and two benzene rings of the adjacent isomorphous chain.

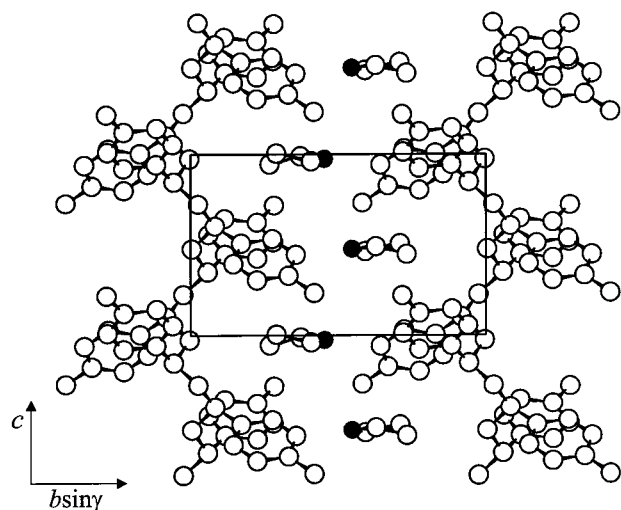


Figure 8. c $bsiny$ projection of the model of packing for the crystal structure of the clathrate form of s-PPMS containing THF in the space group $P2_1/a$. Only the polymer chains with the chain axes at $x/a = 0.25$, $y/b = 0$ and $x/a = 0.25$, $y/b = 1$ and the THF molecules with the barycenter at $x/a = 0.25$ are shown. The oxygen atoms of the THF molecules are indicated by filled circles.

The fractional coordinates of the atoms of the asymmetric unit in the model of Figure 7, for the space group $P2_1/a$, are listed in Table 2. The calculated X-ray intensities are compared in Table 3 to the experimental intensities observed in the X-ray fiber diffraction pattern of Figure 1. A quantitative evaluation of the experimental intensities of the reflections have been obtained from the X-ray powder diffraction pattern, reported in Figure 9A. The quantitative comparison with the calculated intensities gives an agreement factor $R = 19\%$. In Figure 9 the calculated X-ray powder diffraction profile for the model of Figure 7 is compared to the experimental X-ray powder diffraction pattern, after the subtraction of the amorphous halo. A fairly good agreement is apparent.

Concluding Remarks

The crystal structure of the clathrate form of s-PPMS containing THF has been determined by the analysis of the X-ray fiber and powder diffraction patterns and packing energy calculations.

The proposed model could be considered as representative of the crystal structure of the β class clathrates of s-PPMS.¹² Indeed, the crystal structures of clathrate forms of s-PPMS belonging to the β class, that is, containing benzene, cyclohexane, cyclohexanone, and 1,4-dioxane as guest molecules, are probably very similar to that of the clathrate with THF.¹²

It may be interesting to compare the structure of the clathrate form of s-PPMS containing THF with the crystal structures of the clathrate δ forms of s-PS including toluene,⁸ iodine,⁹ and 1,2-dichloroethane.¹¹

A common feature of all these structures is the presence of $s(2/1)_2$ helical chains packed according to the space group $P2_1/a$. Moreover, they are all characterized by the presence of ac layers of chains, composed of 2-fold enantiomorphous helices alternating and close packed along a . The guest molecules are accommodated in cavities between these ac layers of chains succeeding along b .

However, relevant differences concerning the positioning of the guest molecules exist owing to the

Table 3. Comparison between the Calculated Intensities, I_c , for the Model of the Clathrate Form of s-PPMS with THF of Figure 7 and the Experimental Intensities, I_o , Observed in the X-ray Fiber Diffraction Pattern of Figure 1^a

hkl	$d_{obs}(\text{\AA})$	$d_{calc}(\text{\AA})$	I_c^b	I_o^c
010	12.6	12.51	39	m
200	9.19	9.26	72	s
210	8.12	8.15	10	vvw
020	6.33	6.25	26	w
220	5.68	5.66	6	vw
220	4.82	4.81	60	ms
410		4.61	12	
030		4.17	12	
410	4.18	4.11	10	61 m
230		4.08	6	
420		4.07	33	
230		3.57	2	
420		3.44	1	
430		3.41	1	
040		3.12	1	
440		2.82	7	
240		2.38	4	
101		7.07	6	
011		6.55	1	
011		6.55	1	
111	6.37	6.36	89	s
111		6.00	5	
201		5.93	10	
211		5.59	4	
211		5.13	8	
121		4.86	111	125 ms
021	4.90	4.85	4	
021		4.85	4	
301		4.81	6	
311		4.71	91	201 vs
221	4.65	4.56	43	
121		4.54	67	
311	4.33	4.30	90	
321		4.10	12	m
401		3.96	78	79 s
411	3.95	3.95	1	
131		3.71	1	
411	3.60	3.63	20	21 w
421		3.60	1	
511	3.35	3.36	15	w
231		3.24	4	
431		3.10	3	
511		3.10	2	
141	2.98	2.93	12	vw
002	3.99	3.84	55	ne
102		3.76	8	
012		3.67	4	
012		3.67	4	
112		3.64	18	
112	3.56	3.57	53	278 s
202		3.55	225	
212		3.47	37	
212		3.35	8	
022		3.27	3	7 vvww
022	3.28	3.27	3	
302		3.26	1	
312		3.22	10	
222		3.19	5	
122		3.17	1	
312		3.09	21	23 vw
322	3.05	3.01	1	
222		3.00	1	
402		2.95	6	
412		2.95	4	
412	2.85	2.81	3	vvw

^a The Bragg distances, observed in the X-ray fiber diffraction pattern of Figure 1 and calculated for the unit cell with axes $a = 18.8$ Å, $b = 12.7$ Å, and $c = 7.7$ Å and with $\gamma = 100^\circ$, are also shown. ^b Reflections with calculated intensities lower than 1 have been not reported. ^c vs = very strong, s = strong, ms = medium strong, m = medium, w = weak, vw = very weak, vvww = very very very weak, ne = not evaluated.

presence of methyl carbons in the case of s-PPMS. In the clathrate structures of s-PS, guest molecules occupy isolated cavities between the phenyl rings of adjacent

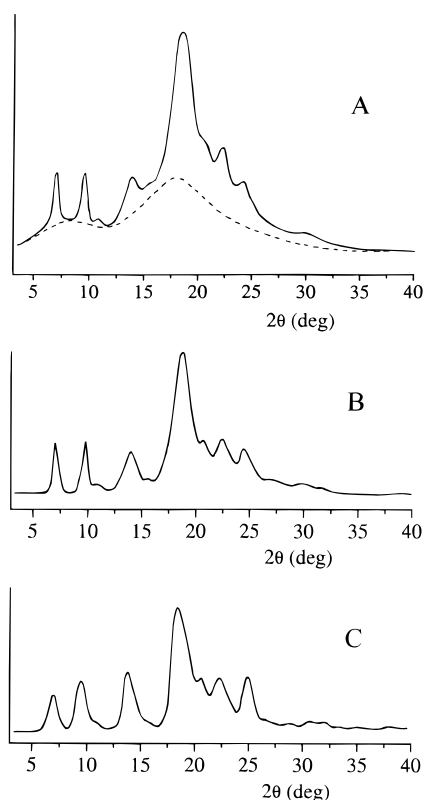


Figure 9. X-ray powder diffraction pattern of the clathrate form of s-PPMS containing THF (A), after the subtraction of the amorphous halo (B), and calculated X-ray powder diffraction profile for the model of Figure 7 (C). The amorphous halo is shown in (A) as a dashed line.

polymer chains along the $a + b$ direction of the unit cell. These cavities are centered at the centers of symmetry of the lattice and, hence, are delimited by enantiomorphous polymer chains. In the present structure of the clathrate form of s-PPMS with THF, the guest molecules occupy cavities around the 2-fold screw axes of the lattice, between the phenyl rings of adjacent s-PPMS

polymer chains along the b axis of the unit cell. At variance with the s-PS clathrate forms, the cavities in this s-PPMS clathrate form are delimited by two isomorphous polymer chains.

Acknowledgment. Financial support from the "Ministero dell'Università e della Ricerca Scientifica e Tecnologica", is gratefully acknowledged.

References and Notes

- (1) Iuliano, M.; Guerra, G.; Petraccone, V.; Corradini, P.; Pellicchia, C. *New Polym. Mater.* **1992**, *3*, 133.
- (2) De Rosa, C.; Petraccone, V.; Guerra, G.; Manfredi, C. *Polymer* **1996**, *37*, 5247.
- (3) Guerra, G.; Dal Poggetto, F.; Iuliano, M.; Manfredi, C. *Makromol. Chem.* **1992**, *193*, 2413.
- (4) Guerra, G.; Iuliano, M.; Grassi, A.; Rice, D. M.; Karasz, F. E.; McKnight, W. J. *Polym. Commun.* **1991**, *32*, 430.
- (5) De Rosa, C.; Petraccone, V.; Dal Poggetto, F.; Guerra, G.; Pirozzi, B.; Di Lorenzo, M. L.; Corradini, P. *Macromolecules* **1995**, *28*, 5507.
- (6) Immirzi, A.; De Candia, F.; Iannelli, P.; Vittoria, V.; Zambelli, A. *Makromol. Chem. Rapid Commun.* **1988**, *9*, 761.
- (7) Guerra, G.; Vitagliano, V. M.; De Rosa, C.; Petraccone, V.; Corradini, P. *Macromolecules* **1990**, *23*, 1539.
- (8) Chatani, Y.; Shimane, Y.; Inagaki, T.; Ijitsu, T.; Yukinari, T.; Shikuma, H. *Polymer* **1993**, *34*, 1620.
- (9) Chatani, Y.; Inagaki, T.; Shimane, Y.; Shikuma, H. *Polymer* **1993**, *34*, 4841.
- (10) De Rosa, C.; Guerra, G.; Petraccone, V.; Pirozzi, B. *Macromolecules* **1997**, *30*, 4147.
- (11) De Rosa, C.; Rizzo, P.; Ruiz de Ballesteros, O.; Petraccone, V.; Guerra, G. *Polymer*, in press.
- (12) Dell'Isola, A.; Floridi, G.; Rizzo, P.; Ruiz de Ballesteros, O.; Petraccone, V. *Macromol. Symp.* **1997**, *114*, 243.
- (13) Cromer, D. T.; Mann, J. B. *Acta Crystallogr.* **1968**, *A24*, 321.
- (14) Yoon, D. Y.; Sundararajan, P. R.; Flory, P. J. *Macromolecules* **1975**, *8*, 776.
- (15) Sundararajan, P. R.; Flory, P. J. *J. Am. Chem. Soc.* **1974**, *96*, 5025.
- (16) Corradini, P.; Napolitano, R.; Pirozzi, B. *Eur. Polym. J.* **1990**, *26*, 157.
- (17) Weiner, P. K.; Kollman, P. A. *J. Comput. Chem.* **1981**, *2*, 287.
- (18) Seip, H. M. *Acta Chem. Scand.* **1969**, *23*, 2741. Almenningsen, A.; Seip, H. M.; Willadsen, T. *Acta Chem. Scand.* **1969**, *23*, 2748.

MA9718964